The Exo70 Subunit of the Exocyst Is an Effector for Both Cdc42 and Rho3 Function in Polarized Exocytosis

Hao Wu,* Courtney Turner,* Jimmy Gardner,* Brenda Temple,†
and Patrick Brennwald*

Departments of *Cell and Developmental Biology and †Biochemistry and Biophysics and R. L. Juliano
Structural Bioinformatics Core, University of North Carolina at Chapel Hill, Chapel Hill, NC 27599-7090

The Rho3 and Cdc42 members of the Rho GTPase family are important regulators of exocytosis in yeast. However, the precise mechanism by which they regulate this process is controversial. Here, we present evidence that the Exo70 component of the exocyst complex is a direct effector of both Rho3 and Cdc42. We identify gain-of-function mutants in *EXO70* that potently suppress mutants in *RHO3* and *CDC42* defective for exocytic function. We show that Exo70 has the biochemical properties expected of a direct effector for both Rho3 and Cdc42. Surprisingly, we find that C-terminal prenylation of these GTPases both promotes the interaction and influences the sites of binding within Exo70. Finally, we demonstrate that the phenotypes associated with novel loss-of-function mutants in *EXO70*, are entirely consistent with Exo70 as an effector for both Rho3 and Cdc42 function in secretion. These data suggest that interaction with the Exo70 component of the exocyst is a key event in spatial regulation of exocytosis by Rho GTPases.

INTRODUCTION

The ability of eukaryotic cells to grow asymmetrically relies on the delivery of lipids and proteins to specific sites on the cell surface. This delivery is largely mediated by the docking and fusion of secretory vesicles with a precisely demarcated region of the plasma membrane. The budding yeast *Saccharomyces cerevisiae* undergoes polarized growth throughout its cell cycle, which makes it an attractive model for studying the regulation of polarized exocytosis and its role in overall cell polarity. An important factor in targeting of secretory vesicles to the plasma membrane is an evolutionary conserved eight-subunit protein complex, known as the exocyst complex, which is composed of Sec3, Sec5, Sec6, Sec8, Sec10, Sec15, Exo70, and Exo84 (for review, see Nelson and Yeaman, 2001; Hsu *et al.*, 2004; Munson and Novick, 2006; Wu *et al.*, 2008).

Both Rab and Rho family small GTPases have been shown to be the upstream regulators of exocyst function in vesicle docking and fusion. The Rab family small GTPase, Sec4, directly interacts with the Sec15 subunit of the exocyst, and it is this interaction that is thought to help link the exocyst complex to the vesicle during docking (Guo *et al.*, 1999). The Rho family small GTPases are also important regulators of polarized exocytosis in yeast. Previous studies have shown that specific conditional mutations in Rho3 or Cdc42 results in actin-independent defects in exocytosis (Adamo *et al.*, 1999, 2001). Although Rho3 and Cdc42 seem to have partially overlapping functions, they are also individually required for polarized exocytosis; loss of function in each GTPase shows a specific set of phenotypes when their secretory function is impaired. The secretory-defective mutant

form of Cdc42, *cdc42-6*, accumulates post-Golgi vesicles only during bud emergence (i.e., small-budded cells) and displays a pronounced defect in secretion of Bgl2 but not in secretion of invertase. In contrast, the secretory defective form of Rho3, *rho3-V51*, accumulates post-Golgi vesicles throughout the cell cycle and has pronounced defects in secretion of both Bgl2 and invertase pathways.

Exo70 has been implicated as a possible effector for Rho3 based on its ability to interact with Rho3 in a GTP-dependent manner (Robinson *et al.*, 1999), and the fact that the interaction of Rho3 with Exo70 is blocked by the presence of the *rho3-V51* effector domain mutation (Adamo *et al.*, 1999). Interestingly, recent studies have identified *exo70* mutant alleles, *exo70-35* and *exo70-38*, that demonstrate a small-bud–specific and Bgl2-specific secretion defect, phenotypes that are remarkably similar to that of *cdc42-6*. These results could suggest a role for Exo70 as a target for Cdc42 during exocytosis, however, a physical interaction between activated recombinant Cdc42 and Exo70 was not detected (He *et al.*, 2007a).

The recent determination of the crystal structure of Exo70 proteins from yeast and mice revealed a conserved rod structure with four domains arranged sequentially from the N to the C terminus (Dong *et al.*, 2005; Hamburger *et al.*, 2006; Moore *et al.*, 2007). Structural similarity also seems to exist between the C-terminal domain of Exo70 and other members of the exocyst complex (Dong *et al.*, 2005; Munson and Novick, 2006; Sivaram *et al.*, 2006). However, despite the conservation in overall structure of yeast and mammalian Exo70, the site of interaction with Rho family GTPases seemed to be quite distinct. Although recombinant Rho3 was found to bind primarily through interactions within the C domain of yeast Exo70, the site of interaction between the mouse Cdc42 homologue TC10 and mouse Exo70 was mapped to the N-terminal AB domains (Chiang *et al.*, 2001).

Recent work has called into question the role of Exo70 as an effector of Rho3 function in exocytosis. Examination of two alleles in *EXO70* suggested that Exo70 function was

required only in small-budded cells (He *et al.*, 2007a), in contrast to studies on Rho3 demonstrating exocytic defects in both small and large budded yeast (Adamo *et al.*, 1999, 2001). More importantly, mutants or deletions in Exo70 predicted to block the interaction with Rho3 in vitro, showed little to no effect on growth or secretory function of *EXO70* (He *et al.*, 2007b; Hutagalung *et al.*, 2009). Together, these results suggested that Exo70 was unlikely to be the effector for Rho3 function in exocytosis.

In the current study, we report a combination of genetic and biochemical examinations to determine the possible role of Exo70 as a target of Rho3 and Cdc42 function in exocytosis. First, we describe the isolation of dominant gain-of-function alleles of *EXO70* that strongly suppress the loss of either Rho3 or Cdc42 function in the exocytic pathway. Second, we describe a biochemical assay using posttranslationally modified forms of Rho3 and Cdc42 to demonstrate that Exo70 has the biochemical properties of a direct effector for both of these GTPases. Interestingly, we found that C-terminally prenylated forms of Rho3 and Cdc42 are able to interact with Exo70 in a manner that is structurally distinct from that of unmodified recombinant Rho3. Finally, we describe the isolation of novel recessive alleles of *EXO70* that demonstrates that the spectrum of phenotypes associated with Exo70 loss of function is in strong agreement with its role as an effector for both Cdc42 and Rho3 function in polarized exocytosis.

MATERIALS AND METHODS

Yeast Strains, Reagents, and Genetic Techniques

Cells were grown in YPD media containing 1% bacto-yeast extract, 2% bacto-peptone, and 2% glucose. The components of the media were from Thermo Fisher Scientific (Waltham, MA). For all assays performed, 25°C was the permissive temperature, whereas 14 and 37°C were used as the restrictive temperatures. Sorbital, sodium azide (NaN₃), N-ethylmaleimide (NEM), β-mercaptoethanol, o-dianasidine, glucose oxidase, peroxidase, Triton X-100, NP-40, and HIS-Select Nickel Affinity Gel were obtained from Sigma-Aldrich (St. Louis, MO). Zymolyase (100T) was from Seikagaku (Tokyo, Japan). Bovine serum albumin, yeast nitrogen base, raffinose galactose, and 5-fluoro-orotic acid (5-FOA) were from United States Biologicals (Swampscott, MA). Glutathione-Sepharose beads and protein A beads were from GE Healthcare (Little Chalfont, Buckinghamshire, United Kingdom). Guanosine 5′-O-(3-thio)triphosphate (GTPγS) and guanosine diphosphate (GDP) were from Roche Applied Science (Indianapolis, IN). Secondary antibodies for Odyssey imaging system were from LI-COR Biosciences (Lincoln, NE) and Invitrogen (Carlsbad, CA). Rabbit anti-mouse antibody was from Jackson ImmunoResearch Laboratories (West Grove, PA). Formaldehyde (37%), glutaraldehyde, and Spurr's resin were from Electron Microscopy Sciences (Ft. Washington, PA). The TNT in vitro translation system for polymerase chain reaction (PCR) products was from Promega (Madison, WI). L-[³⁵S]Methionine was from PerkinElmer Life and Analytical Sciences (Boston, MA). Mevalonic acid was from Sigma-Aldrich. The bead beater for making yeast lysate is from BioSpec Products (Bartlesville, OK). Transformations for suppression analysis were performed using the lithium acetate method described in Guthrie and Fink (1991). Strain crossing, tetrad dissection, diploid sporulation, and mating-type determination were performed as described by Guthrie and Fink (1991).

Dominant Suppressor Screen for Exo70 Dominant Mutants

The *EXO70* dominant mutants in this study were generated by Error-prone PCR as described below. Fifty nanograms of digested vector and 3 μl of PCR reaction were transformed into the *RHO3* plasmid shuffle strain (*rho3Δ::LEU2;his3-Δ200, ura3-52;leu2-3112; pRS316-RHO3,URA3,CEN,*) and the *cdc42-6* strain (BY648 α, *cdc42-6, leu2,3-112; ura3-52*). CEN HIS3 vector was used for *RHO3* plasmid shuffle strain, and CEN URA3 vector was used for *cdc42-6* strain. Transformants were first grown on selective media for 2 d and then replica plated onto 5-FOA plates at 30°C for the *RHO3* plasmid shuffle strain and YPD plates at 32°C for *cdc42-6* mutant strain. Colonies from the restrictive conditions were grown in liquid media for plasmid recovery. The plasmids were retransformed into *RHO3* plasmid shuffle strain and *cdc42-6* mutant strain to confirm that the plasmids were responsible for the gain of function phenotype. From 6030 transformants from the *RHO3* plasmid shuffle strain, we isolated three plasmids that suppressed the *rho3Δ* at 30°C. From 5660 transformants in the *cdc42-6* strain, we isolated 38 plasmids that had the ability to suppress the temperature sensitivity of the *cdc42-6* mutant at 32°C.

Isolation of Novel Exo70 Mutants by Random Mutagenesis

The *EXO70* mutants isolated in this study were generated by GeneMorph II random mutagenesis kit (Stratagene, La Jolla, CA). Then, 50 ng of plasmid pRS315 Exo70 was used as a template for PCR reaction performed under conditions that produce 0–4.5 mutations/kb (low frequency of mutagenesis) according to the manufacturer's protocol. Oligonucleotide primers were designed to generate mutagenized PCR products containing the *EXO70* open reading frame flanked by 629 base pairs of 5′ and 295 bp of 3′ sequence. The *EXO70* gap repair vector (BB1673) was digested with BamHI and XbaI. Then, 50 ng of digested vector were cotransformed with 3 μl of PCR product into *EXO70* plasmid shuffle strain (BY861: *exo70Δ::HIS3;his3-Δ200, ura3-52;leu2-3112; pRS316-EXO70,URA3,CEN*). Transformants that repaired the gapped plasmid by homologous recombination were selected at 30°C on SD plates for 2 d. Transformants that could lose the wild-type plasmid pRS316 Exo70 were selected by replica plating onto synthetic minimal media containing 5-FOA while simultaneously selecting for the temperature sensitivity by incubation of replica plates at 37, 25, 17, and 14°C.

From 10,396 colonies, 40 colonies exhibited temperature sensitivity and 57 colonies exhibited cold sensitivity. Plasmids from these colonies were isolated and transformed back into the original *EXO70* plasmid shuffle strain (BY861) to confirm that the plasmids were responsible for the temperature sensitivity and cold sensitivity. One plasmid was found to give rise to a cold-sensitive phenotype (*exo70-188*) and one plasmid was found to have a temperature sensitive phenotype (*exo70-113*). Sequence analysis demonstrated that the cold-sensitive mutant, *exo70-188*, contained the three mutations S305G, T523P, and L621I. Analysis of the temperature-sensitive allele *exo70-113* contained two mutations: N79K and incorporation of a stop codon at Y327 leading to truncation of the C-terminal half of the predicted protein.

Genetic Analysis of Mutants

To study the phenotypes of *exo70-188* and *exo70-113* alleles as the only copy of *Exo70*, the constructs were integrated into the chromosome of the diploid strain BY841 (*a/α; exo70Δ::HIS3/EXO70; his3Δ200/his3Δ200; ura3-52/ura3-52; leu2-3112/leu2-3112*) at the *EXO70* locus. Transformants were sporulated and tetrads were dissected with the use of a micromanipulator on YPD plates. The plates were grown at 25°C and the haploid progeny were analyzed for the presence of the mutants (scored as *KanR*), the absence of the wild-type *EXO70* (scored as *his3Δ200*), viability, and conditional growth defects.

Electronic Microscopy

The exo70-188 and exo70-113 mutants were grown overnight to mid-log phase in YPD media. Half of the cultures were shifted to restrictive temperature for various time periods. The *exo70-188* mutant was shifted to a 14°C water bath shaker for 9 h, where the *exo70-113* mutant was shift to 37°C water bath shaker for 1.5 h. Shifted and unshifted cells were processed as described previously (Adamo *et al.*, 1999).

Invertase Assay and Bgl2 Assay

The *EXO70, exo70-188, exo70-113, rho3-V51*, and *sec6-4* cells were grown overnight to mid-log phase at 25°C in YPD liquid media. For the cold-sensitive strains *exo70-188* and *rho3-v51*, the cells were preshifted to the restrictive temperature of 14°C for 1 h. After the preshift, one sample was taken as T₀ and the rest of the cells were shifted to prechilled YP media containing 0.1% glucose for 9 h. Samples after the temperature shift were collected as Tfinal. For temperature-sensitive alleles *exo70-113 and sec6-4*, the cells were directly shifted to warm YP media containing 0.1% glucose for 1.5 h at 37°C. Samples collected before and after the temperature shift were collected as T₀ and Tfinal, respectively.

After the temperature shift, the cells were spheroplasted and the internal and external fractions were separated. Samples were processed as described previously (Adamo *et al.*, 1999; Lehman *et al.*, 1999). The percentage of internal invertase accumulation is calculated by: Δinternal/(Δ internal + Δ external).

To analyze the accumulation of Bgl2 enzyme, cells were grown in YPD media overnight to mid-log phase. The *exo70-188* mutant cells were then shifted to a 14°C water bath shaker for 10 h. The *exo70-113* mutant cells were shifted to 37°C water bath shaker for 2 h. The cells were spheroplasted, and the internal and external fractions were separated. Samples were then boiled with 6x sample buffer for 5 min at 95°C. Internal and external samples were then subjected to SDS-polyacrylamide gel electrophoresis (PAGE) gel, transferred to nitrocellulose, and blotted with affinity purified anti-Bgl2 antibody at a dilution of 1:100. Quantification of the western blots was analyzed by Odyssey infrared imaging system (LI-COR Biosciences).

Construction of pGEX-6His Vector and Protein Expression, Purification, and Quantification

The pGEX6p1 vector was digested with NotI and SalI. An additional PreScission enzyme site and a 6-histidine tag were generated by fusion PCR reaction and introduced into the Not1 and Sal1 sites of pGEX6p1 to create pGEX-6P6H (pB1579). The resulting plasmid contained an N-terminal glutathione transferase (GST) tag and a C-terminal 6xHis tag flanking the polylinker and was used to

create the following GST-fusion constructs: GST-Sec9 (aa 402-651), GST-Ste20 (aa 314-432), GST-Exo70 (aa 1-623), GST-Exo70-1521, GST-Exo70-DC. GST-Sec4 (1-211), GST-Rho1 (aa 1-205), GST-Rho2 (aa1-188), GST-Rho3 (aa 1-227), GST-Rho4 (aa 1-287), and GST-Cdc42 (aa 1-187) were subcloned into pGEX-6p-1 vector. All constructs were confirmed by sequencing and protein expression was performed in *Escherichia coli* BL21 cells. Cells were grown at 37°C in Terrific broth medium to an OD_{599} 2.0–2.5. Cells were shifted to 25°C, and protein expression was induced with 0.1 mM isopropyl β-D-thiogalactoside for 3 h at 25°C. To maximize protein solubility, GST-Exo70-ABD was induced at 22°C for 4 h. Cells were pelleted and frozen at −80°C until lysis.

6xHis-tag purification was performed by binding the bacteria lysate to HIS-Select Nickel Affinity Gel (Sigma-Aldrich) and then eluting with 500 mM imidazole. The 6xHistidine eluates were then incubated with glutathione-Sepharose beads at 4°C for 1 h, and the beads were washed with wash buffer (20 mM Tris, pH 7.5, 120 mM NaCl, and 1% Tween 20) to remove unbound proteins. Protein concentration was determined by comparison to purified protein standards after SDS-PAGE and Coomassie Blue staining. Quantification of Coomassie Blue-stained gels was performed by Odyssey infrared imaging system (LI-COR Biosciences).

In Vitro Binding Assays

Glutathione beads carrying GST,GST-Rho1-4, GST-Cdc42 were washed with 20 mM Tris-HCl, pH 7.5, 150 mM NaCl, and 1 mM dithiothreitol (DTT) and were incubated in 20 mM Tris, pH 7.5, 150 mM NaCl, 5 mM EDTA, and 1 mM DTT in the presence of 100 μM GTPγS for 30 min at 25°C. MgCl$_2$ was added to a final concentration of 25 mM and incubated 30 min at 25°C. Binding assays were performed in binding buffer (20 mM Tris-HCl, pH 7.4, 150 mM NaCl, 5 mM MgCl$_2$, 1 mM DTT, and 0.5% Triton X-100). The final concentrations of GST, GST-Rho1-4, and GST-Cdc42 in the binding reactions were 2 μM. Samples were incubated at 4°C for 2 h. The beads were washed five times with binding buffer and boiled with 85 μl of sample buffer at 95°C for 5 min. Samples were subjected to SDS-PAGE and autoradiography.

Generation of Yeast Cell Lysate

RHO3L74, RHO3N30, CDC42L61, CDC42N17, and *RHO1L68* were amplified by PCR reaction and subcloned behind the GAL1 promoter in a *LEU2* integrating vector (BB24, pRS305 with GAL1 promoter). The vector was linearized by digesting with BstXI restriction enzyme and transformed into a Gal$^+$ strain BY17 (*a; GAL1; leu2-3112; ura3-52*). Yeast strains were first grown in YP 3% raffinose overnight at 30°C to mid-log phase of OD 1–1.5. The small GTPases were induced by adding final concentration of 1% galactose for two more doublings (4 h) at 30°C. Cells were pelleted by centrifugation at 5000 rpm for 5 min and washed with double-distilled H$_2$O. Pellets were immediately frozen on dry ice. Frozen pellets were lysed with a bead beater from BioSpec Products. The optimal wet weight for the small chamber was 5–6 g. The pellet was beaten for 1 min followed by a 3-min pause for five cycles. Lysate was then subjected to centrifugation for 10 min at 17,000 × g, followed by ultracentrifugation at 100,000 × g for 30 min. The protein concentration of the lysate was measured by a Bradford assay (Bradford, 1976). Each lysate was normalized to ~25 mg/ml total protein concentration and frozen on dry ice.

GST Pull-Down from Yeast Cell Lysate

All recombinant proteins were present at a final concentration of 3 μM. Cell lysates were prepared for GST pull-down experiments as described above and incubated with each fusion protein bound to glutathione-Sepharose beads for 1.5 h at 4°C. The beads were washed five times with lysis buffer (20 mM Tris-HCl, pH 7.5, 120 mM NaCl, 10 mM MgCl$_2$, 1% Tween 20, and 1 mM DTT), and boiled at 95°C for 5 min. Samples were subjected to SDS-PAGE gel, and analyzed by immunoblotting with Rho1, Rho3, and Cdc42 monoclonal antibody. Quantification of Western blots was performed with Odyssey infrared imaging system (LI-COR Biosciences).

In Vitro Prenylation Assay

The coding sequence of Rho3 was amplified by PCR reaction using standard PCR conditions. A common TNT-T7 primer was designed especially for in vitro transcription/translation, which contains a promoter and a Kozak consensus sequence (GCATGGATCCTAATACGACTC ACTATA GGA CAA CAG CCA CCA TGG GA). Then, 10 μl of rabbit reticulocyte lysate, 0.5 μl of [^{35}S]methionine, and ~200 ng of amplified DNA (7 μl PCR reaction) were first incubated at 30°C for 1.5 h, and 5 mM mevalonic acid was added to the reaction for 6 h. The mevalonic acid was prepared as described previously (Hancock, 1995). At the end of the in vitro translation and prenylation reaction, 75 μl of binding buffer (20 mM Tris-HCl, pH 7.5, 120 mM NaCl, 10 mM MgCl$_2$, 1% Tween 20, and 1 mM DTT) was added to each translation mix and incubated with 15 μl of GST-Sec9, GST-Exo70, or GST-Ste20 for 2 h at 4°C. The beads were washed five times with binding buffer and boiled with 85 μl of sample buffer at 95°C for 5 min. Samples were subjected to SDS-PAGE, and the gels were quantitated with Storm PhosphorImager with ImageQuant software (GE Healthcare).

Immunoprecipitation of the Exocyst Complex

Strains containing dominant mutants of Exo70 as the only source of Exo70 were grown to mid-log phase in SC media at 30°C and shift to YPD rich media for 1.5 h. The 300 OD units of cells were pelleted and washed with cold 10:20:20 buffer (10 mM Tris, pH 7.5, 20 mM NaN$_3$, and 20 mM NaF). Pellets were resuspended in lysis buffer [20 mM piperazine-N,N′-bis(2-ethanesulfonic acid) (Pipes) pH 6.8, 120 mM NaCl, 1 mM EDTA, and 1 mM DTT]. Cells were lysed by bead beating in lysis buffer and extracted by adding 5× extraction buffer (20 mM Pipes, pH 6.8, 120 mM NaCl, 1 mM EDTA, 1% NP-40, and 1 mM DTT). Lysates were cleared by centrifugation at 14,000 rpm for 9 min and normalized for total protein concentration by Bradford assay (Bradford, 1976). The supernatants were added to prewashed protein beads for 30 min on ice to reduce nonspecific binding and then spun for 5 min at 14,000 rpm. Input samples were collected, and the remaining lysate was placed in fresh Eppendorf tubes in the presence of 9E10 monoclonal anti-myc antibody. Samples were incubated on ice for 45 min, and then we added 2 μl of rabbit anti-mouse antibody followed by incubation on ice for another 30 min. Lysate-antibody mix was then added to fresh, prewashed protein A beads for 60 min on ice. Samples were washed five times with wash buffer (20 mM Pipes, pH 6.8, 120 mM NaCl, 1 mM EDTA, and 1% NP-40) and boiled at 95°C for 5 min with 2× sample buffer. Input and bound fractions were analyzed by SDS-PAGE gels and Western blotting. Quantitation of Western blots was performed by Odyssey infrared imaging system (LI-COR Biosciences).

RESULTS

Isolation of Dominant Gain-of-Function Alleles of EXO70

We have suggested previously a model for localized stimulation of exocytosis by the guanosine triphosphate (GTP)-bound forms of Rho3 and Cdc42. For Rho3, we proposed this activation would involve interaction with the Exo70 subunit of the exocyst complex, whereas the effector for Cdc42 was unknown (Roumanie *et al.*, 2005; Wu *et al.*, 2008). Using other Rho-effectors such as formins, Wiskott–Aldrich Syndrome protein, or p21-activated kinase kinases, as a model, one might expect that downstream activation would involve "relief of autoinhibition," i.e., that binding of Rho3-GTP to the Exo70 subunit of the exocyst would activate this complex by blocking inhibitory interactions between Exo70 and other components of the complex, thus reorganizing the complex into a more active form (Wu *et al.*, 2008). A prediction of this model is that mutations in Exo70 that block or perturb inhibitory interactions of Exo70 within the exocyst should act as "activated" or gain-of-function alleles and would behave genetically as dominant-suppressors of loss of Rho3 function. Furthermore, if Rho3 and Cdc42 share a common pathway in regulating exocyst function then mutants that suppress loss of Rho3 function in exocytosis should also suppress loss of Cdc42 function in exocytosis.

To test these predictions, we performed two independent screens to look for dominant suppressing forms of *EXO70*. One screen made use of the *rho3Δ* mutant, which is sensitive to increased gene dosage of several components of the exocytic apparatus (Matsui and Toh, 1992; Imai *et al.*, 1996; Lehman *et al.*, 1999). The other screen made use of the *cdc42-6* mutant that has a highly allele-specific defect in exocytosis that genetically overlaps with that of Rho3 (Adamo *et al.*, 2001). *EXO70* was randomly mutagenized by PCR amplification and introduced into the mutant yeast strains by cotransformation with a gap-repair plasmid containing the flanking sequences of the *EXO70* gene (see *Materials and Methods*). Approximately 6000 transformants were assayed from each strain and ~45 plasmids containing dominant suppressing forms of *EXO70* were isolated from both screens. Our initial work focused on the 41 strongest suppressors. When we examined the strongest 16 *EXO70* dominant suppressors isolated from the *cdc42-6* screen in the *rho3Δ* strain, we found that they also strongly suppressed (Supplemental Figure S1). When we examined the ability of the 3 strongest *EXO70* dominant suppressors isolated from the *rho3Δ* screen to suppress *cdc42-6* we found that all but

Figure 1. Dominant mutations of *EXO70* are able to suppress *rho3Δ* and *cdc42-6* mutants. (A) The structure of *S. cerevisiae* Exo70 (residues 62-623) is in a transparent surface representation with mutant residues in a space-filing model. The domains are labeled A–D from the N terminus to the C terminus. The arrows point to the residues involved in Exo70 gain of function mutations. Residues colored in blue represent highly conserved residues, residues colored in yellow represent residues conserved only within fungi, and residues colored in pink represent variable residues. Three residues, I114, G388, and N479, are buried within the structure, whereas the remaining seven mutations are surface-exposed residues. The image was generated using the PDB file 2B1E. (B) The gain-of-function mutations of *EXO70* are capable of suppressing a *rho3Δ* and the *cdc42-6* mutant at the restrictive temperature. Dominant mutants of *EXO70* were transformed into a *RHO3* plasmid shuffle strain and a *cdc42-6* strain on *CEN* plasmids. The growth of three independent transformants is shown for each *EXO70* mutant in both mutant strains under restrictive conditions. (C) The *EXO70* dominant mutations can function as the sole copy of Exo70 in the cell. The dominant mutations were introduced into the *EXO70* plasmid shuffle strain on a *CEN-LEU2* plasmid. Three individual colonies were picked to show the growth of each *EXO70* mutant under restrictive conditions when the plasmid containing wild-type *EXO70-URA3* was lost by counterselection on 5-FOA plates. (D) *EXO70* dominant mutants express similar amounts of Exo70 compared with wild-type cells. Whole cell lysate were made from the strains containing Exo70 gain of function mutants as the only source of *EXO70* in the cell. The lysates were subjected to SDS-PAGE analysis and blotted with anti-Myo2 and anti-Exo70 antibodies.
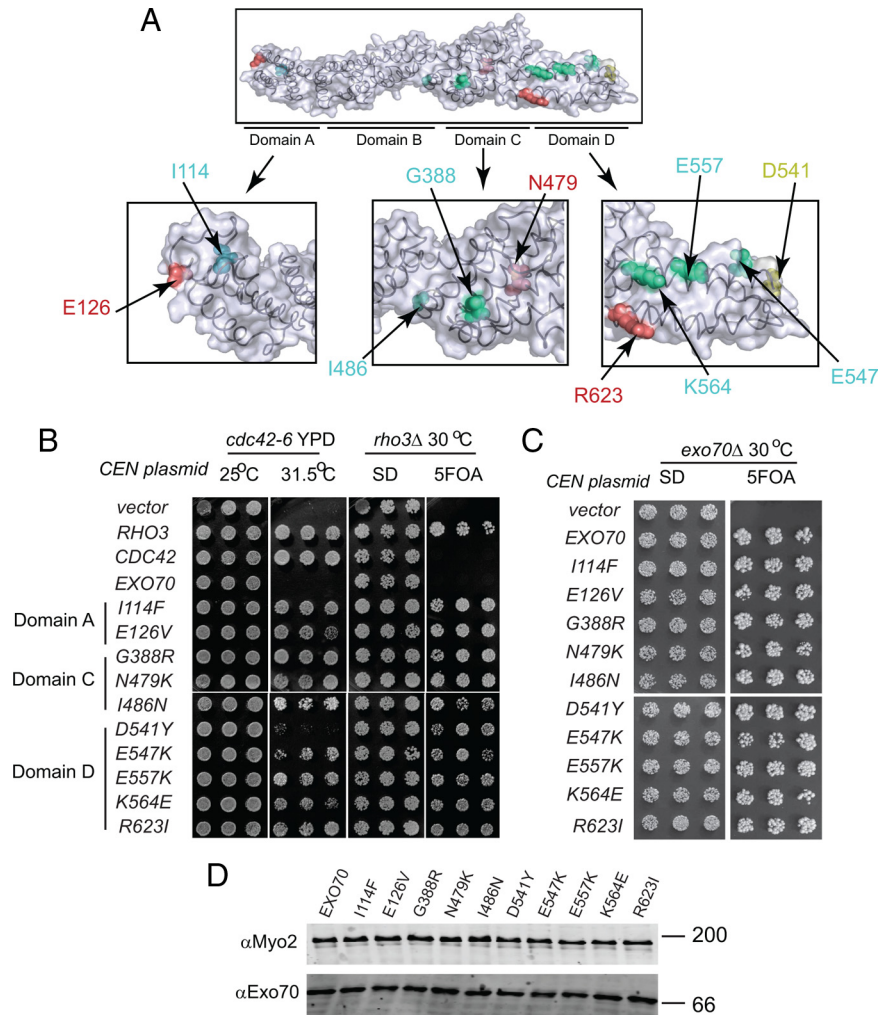
one of these also strongly suppressed *cdc42-6* (Supplemental Figure S1A). We also examined all 16 mutants in *rho3Δ*, *rho4Δ* and found they all strongly suppressed (Supplemental Figure S1B). Therefore, each of these two genetic screens appeared to be selecting for mutants in *EXO70* with similar properties. The ability of these suppressors to potently suppress growth defects associated with both *rho3* and *cdc42* loss-of-function strongly supports the idea that Exo70 is a functionally important downstream target of regulation by both of these Rho GTPases.

Sequence analysis of 41 of the strongest suppressors identified an average of five to eight coding sequence changes per dominant suppressing allele. This was not unexpected, as the predicted frequency of mutations for the amplifying conditions used was 1- to 2-base pair changes/kb. To identify specific amino acid substitutions linked to the suppression activity, we scanned the mutant sequences for missense mutations that appeared in two or more of the suppressing plasmids. This identified 10 single residue mutations as candidate residues to confer dominant suppression on Exo70. These mutations were then prepared as single residue changes and tested for dominant suppression in *rho3Δ* or *cdc42-6* (Figure 1).

The placement of the dominant gain-of-function mutations in the crystal structure of yeast Exo70 revealed a number of possible sites of regulation. Three residues, I114, G388, and N479, are buried within the structure. The other seven mutations are all surface exposed residues. Charged resi-

dues at the D domain form two patches—D541 and E547 form one patch and E557, K564, and R623 form another patch. N479 and G388 are located at the interface of the B and C domains, which potentially cause rearrangements of the two domains relative to each other within the structure of Exo70. An alignment of Exo70 protein sequences from yeast, mouse, worm, and fly is shown in Supplemental Figure S2. The site of each dominant suppressing mutation is indicated on the alignment along with the overall conservation of each residue. As can be seen in Supplemental Figure S2, six of the dominant suppressing mutations occur in highly conserved residues (I114, N479, D541, E547, E557, K564)—four of which reside in a single helix (H17) within the Exo70 crystal structure—suggesting this may be a "hot spot" for activation of the exocyst by Exo70. Together, however, the results of this screen overall suggest that there are likely to be multiple, structurally distinct mechanisms by which *EXO70* gain of function can be achieved.

One possible mechanism for activation of the exocyst complex by the gain-of-function mutants is by effecting the assembly or disassembly of individual subunits of the complex. To determine whether this was the case, we examined the assembly state of the exocyst complex in the presence of the *EXO70* gain-of-function alleles as the sole source of Exo70 in the cell. We immunoprecipated wild-type and mutant exocyst complexes using strains containing a C-terminally myc-tagged form of *SEC8* (Sec8-myc) and anti-myc antibody-coated beads
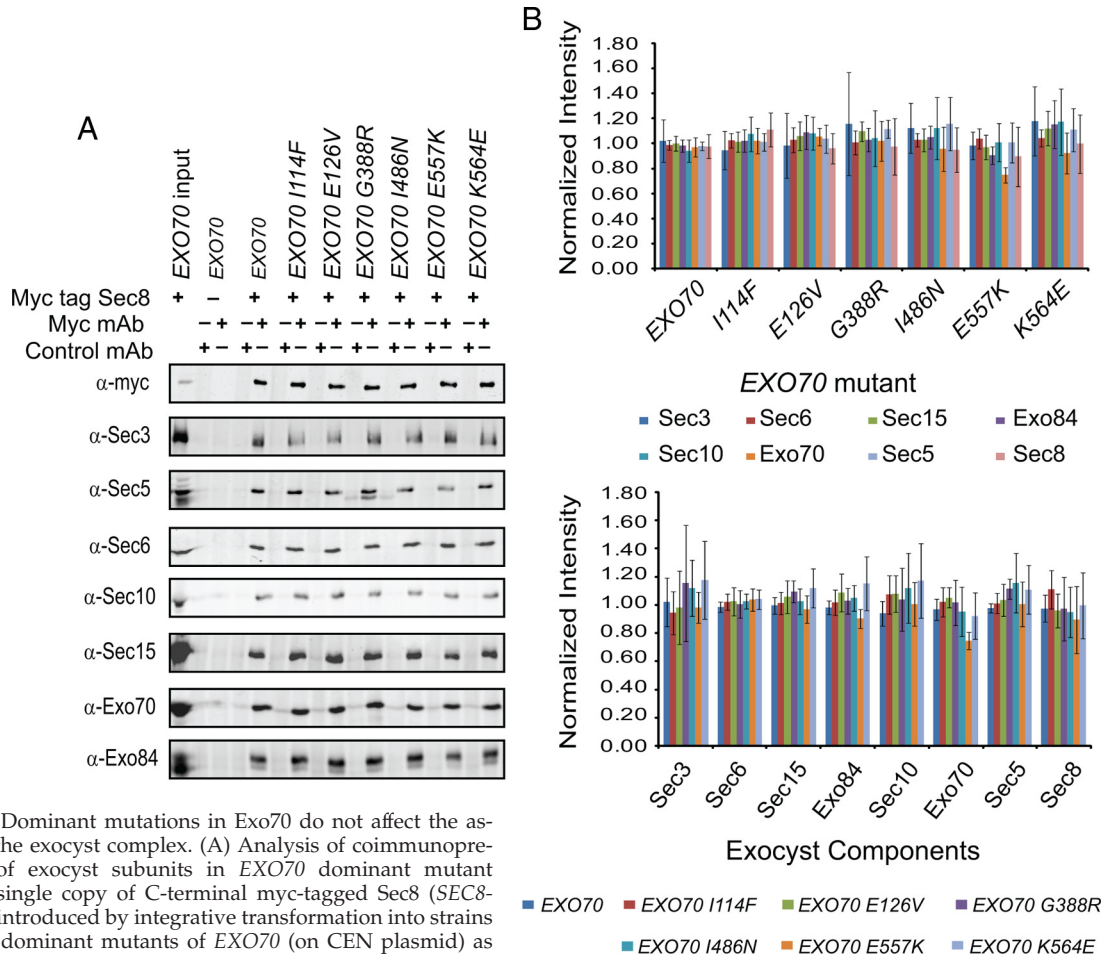
Figure 2. Dominant mutations in Exo70 do not affect the assembly of the exocyst complex. (A) Analysis of coimmunoprecipitation of exocyst subunits in *EXO70* dominant mutant strains. A single copy of C-terminal myc-tagged Sec8 (*SEC8-MYC*) was introduced by integrative transformation into strains containing dominant mutants of *EXO70* (on CEN plasmid) as the only source of Exo70 in the cell. Cells were grown, lysed, and subjected to native immunoprecipitations with myc antibody to analyze the integrity of the exocyst complex (see *Materials and Methods* for details). We loaded 12% of total lysate and 10% of myc immunoprecipitate on SDS-PAGE gel for Western blot analysis with antibodies against each exocyst components. (B) Quantitation of Western blots described in A were performed by Odyssey infrared imaging system. Top, quantitation of each individual subunit in the Sec8 Myc immunoprecipitation organized by strain. Bottom, comparison of wild type and each gain of function strain organized by individual subunit. Error bars represent SD of four independent experiments.

(TerBush and Novick, 1995), and we assayed for the presence of the other exocyst subunits by quantitative Western blot analysis. As can be seen in Figure 2, all six of the gain-of-function alleles of *EXO70* examined resulted in nearly identical amounts of exocyst subunits being coprecipitated with Sec8-myc. An exception was the *EXO70-E557K* allele which had a small (~25%) reduction in the mutant Exo70 protein coprecipitated with the complex. However, this seems to mirror a similar small reduction in the overall steady-state amounts of this protein in the *EXO70-E557K* cells rather than an effect on assembly or disassembly of the complex. Because the activation of the exocyst complex with these gain-of-function mutants seems to mimic the effect of Rho3/Cdc42 activation, these data suggest that assembly and/or disassembly of the complex is unlikely to be the central means of regulation by Rho3 and Cdc42 GTPases.

The GTP-bound Forms of Rho3 and Cdc42, Produced in Yeast, Interact with Exo70

The dominant suppressor analysis described above suggests that Exo70 is probably a critical downstream target of both Rho3 and Cdc42 regulation of exocytosis. However, work using recombinant forms of these GTPases produced in *E. coli* is

inconsistent with this notion. First, recombinant Cdc42-GTP fails to show any detectable interaction with Exo70 (Figure 3A; He *et al.*, 2007a). Recombinant Rho3 does interact with Exo70 in a GTP-dependent and effector domain-dependent manner (Figure 3, A and B) but with relatively low affinity (Hamburger *et al.*, 2006). Second, mutations or deletions in Exo70 that severely diminish this interaction in vitro fail to recapitulate growth or secretory defects associated with either the *rho3-V51* or *cdc42-6* cells (He *et al.*, 2007b; Hutagalung *et al.*, 2009). Because nearly all small GTPases are subjected to posttranslational modifications that do not occur after expression in *E. coli*, we sought to determine whether we could detect an interaction after their overexpression in yeast. To determine the nucleotide dependence of this interaction, we made use of mutant forms of Rho3 and Cdc42 which are predicted to "lock" the GTPases in the either the GTP-bound conformation (Rho3-L74 or Cdc42-L61) or GDP-bound conformation (Rho3-N30 or Cdc42-N17). The nucleotide-locked forms of each GTPase were overexpressed (~20-fold) using an inducible *GAL1/10* promoter, and the induced cells were used to make detergent lysates (see *Materials and Methods*). These lysates were then used in binding experiments with purified full-length Exo70 fused to GST or various control GST-fusion proteins. A GST-fusion containing

Figure 3. Exo70 binding to Rho GTPases expressed in *E. coli* or yeast. (A) Yeast Rho GTPases (Rho1-4, and Cdc42) were expressed, purified from bacteria as GST-fusion proteins, and immobilized on glutathione-Sepharose beads. The beads were preloaded with GTP and bound to radiolabeled in vitro-translated full-length Exo70 and the CRIB domain of Ste20. Input represents 1% binding. (B) The V51 mutation in the effector domain of Rho3 (Rho3V51) abolishes the interaction between Rho3 and Exo70 in vitro. Recombinant GST-Rho3 and GST-Rho3V 51 were purified from bacteria and the immobilized GST-fusion protein was preloaded with GTPγS or GDP. Input represents 1% binding. (C) Exo70 interacts with GTP-locked Rho3 and Cdc42 obtained from a yeast lysate. GST-fusion proteins were purified from bacteria and immobilized on glutathione-Sepharose beads. GTP or GDP locked forms of small GTPases were expressed behind a galactose inducible promoter in yeast. Lysates obtained from these strains were used in the binding experiments (see *Materials and Methods*). The input represents 2.5% binding. Bound material was analyzed by Western blot using monoclonal anti-Rho3, anti-Rho1, and anti-Cdc42 antibodies. Because of the extremely strong binding to Ste20 binding reactions with Cdc42-L61 (but not Rho3, Rho1) were diluted 20-fold before loading to improve quantitation and avoid obscuring the adjacent lanes. (D) The interaction between Exo70 and Rho3/Cdc42 obtained from yeast is sensitive to mutations in the effector domain of the two GTPases. The *rho3V51, L74* and *cdc42-6* effector domain mutations (*cdc42-L29, V31, H32,* and *L61*) were expressed behind a galactose inducible promoter in yeast. Lysates generated from the overexpressing yeast strains were subjected to binding experiments as described above. (E) Bar graphs represent quantitation of the blots using the Odyssey infrared imaging system. Data were analyzed by two-tail Student's *t* test with error bars representing SD from four independent experiments.
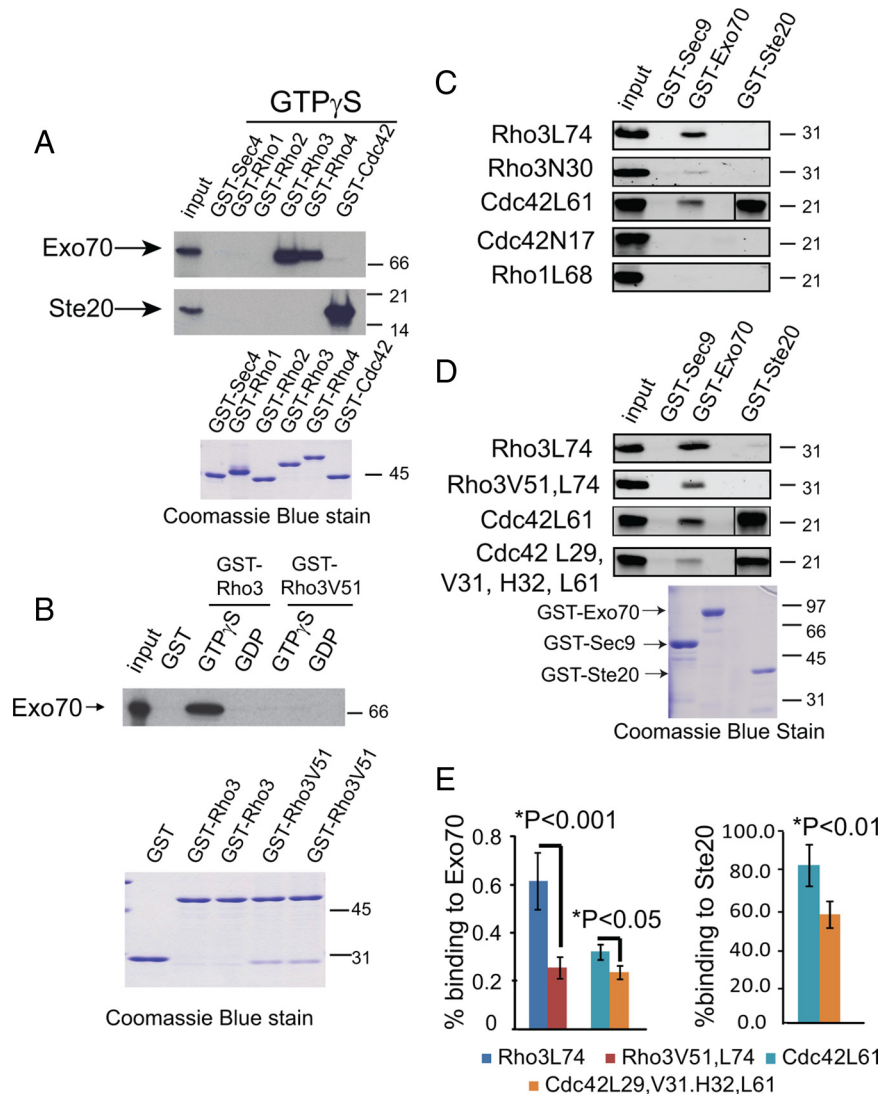
the C-terminal CRIB domain of the Ste20 protein was included as a positive control for Cdc42. As can be seen in Figure 3C, both the GTP-locked forms of Rho3 and Cdc42, Rho3-L74 and Cdc42-L61, are specifically pulled down by GST-Exo70 and this binding is nearly completely lost in lysates overexpressing the GDP-mutant forms of Rho3 and Cdc42, Rho3-N30, and Cdc42-N17. In contrast to Rho3 and Cdc42, no binding to Exo70 was detected with lysates overexpressing GTP-locked Rho1, indicating that the interaction with Exo70 is specific to Rho3 and Cdc42.

Because specific mutations in the effector domain of Rho3 and Cdc42 have been described (*rho3-V51* and *cdc42-6*) that strongly interfere with the function of these GTPases in promoting exocytosis (Adamo *et al.*, 1999, 2001), we examined the effects of these mutations on binding to Exo70. The effector mutations were incorporated in the context of a GTP-locked form of the GTPases and overexpressed as described above. As can be seen in Figure 3D, the presence of the V51 mutation causes a severe defect in binding to Exo70. The *cdc42-6* mutant contains a cluster of three mutations (L29, V31, and H32) in the effector domain that are critical to the temperature-sensitive defect in exocytosis (Adamo *et al.*, 2001). The inclusion of these mutations in the context of a GTP-

locked form of Cdc42, causes a significant loss of binding to GST-Exo70 (Figure 3D). Therefore, the Exo70 binding with Rho3 and Cdc42 from yeast lysates presented here shows clear specificity, nucleotide-dependence, and effector domain sensitivity expected for a bona fide assay for GTPase:effector interaction.

Prenylation of Rho3 and Cdc42 Is an Important Determinant for Binding to Exo70

One possible explanation for the results described above is that a eukaryotic-specific posttranslational modification such as prenylation of the C-terminal CAAX might be required for binding with Cdc42 and Exo70. We therefore produced lysates of GTP-locked forms of Cdc42 and Rho3 with a mutation at the C-terminal Cysteine (in the CAAX motifs) and monitored the effect on binding to recombinant effector proteins. The results are shown in Figure 4. As expected the CAAX (C188A) mutation had no effect on binding of Cdc42-L61 to GST-Ste20. In contrast, a dramatic loss of binding to Exo70 was observed for Cdc42-L61,A188, suggesting that C-terminal prenylation of Cdc42 is a prerequisite for binding. Interestingly, we found that mutation of the CAAX motif of activated Rho3 (L74,A228) also resulted in a dramatic loss of binding to GST-Exo70, suggesting that the binding detected
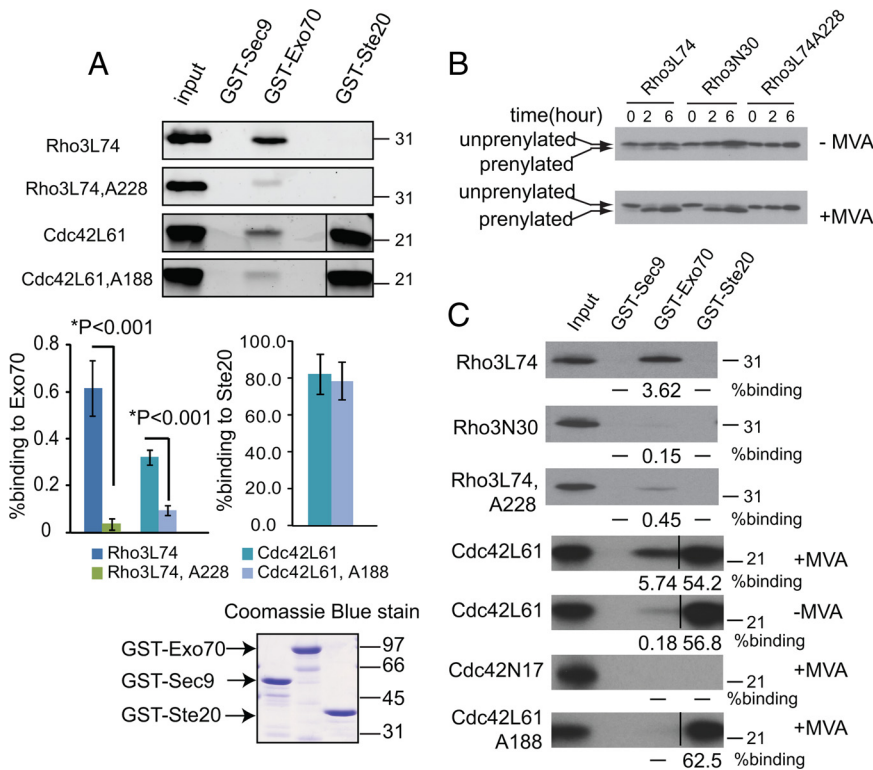
Figure 4. Prenylation of Rho3 and Cdc42 promotes the GTP-dependent interaction with Exo70. (A) The interaction between Exo70 and the two Rho GTPases, Rho3 and Cdc42, from yeast lysate is dependent on C-terminal prenylation. Activated forms of Rho3 and Cdc42 (Rho3L74, Cdc42L61) containing a cysteine-to-alanine mutation in the CAAX box (Rho3-L74, A228, and Cdc42-L61, A188) were overexpressed in yeast. Lysates were prepared in parallel for these mutants and for the activated GTPases containing the intact CAAX motif (Rho3-L74 and Cdc42-L61) and used in binding experiments (see *Materials and Methods*). Ste20 binding assays with Cdc42 (but not Rho3) were diluted 20-fold before loading. As expected, Ste20 binding was unaffected by the prenylation site mutation. Bar graphs represent quantitation of binding experiment with error bars representing SD of three independent experiments. Coomassie Blue staining of the GST-fusion proteins used in the experiment is shown below the quantitation. (B) In vitro prenylation of Rho3 results in a change in mobility and is stimulated by addition of mevalonic acid to reticulocyte lysate. Rho3 was in vitro translated in rabbit reticulocyte lysates (see *Materials and Methods*) and then subjected to extended incubation (for the time shown) in the presence or absence of mevalonic acid (±MVA). The appearance of a faster migrating species appears during the extended incubation and is strongly stimulated by the addition of mevalonic acid and is abolished by mutation of the CAAX box cysteine 228 to alanine. (C) The interaction between Exo70 and Rho3 and Cdc42 produced in reticulocyte lysates is dependent on C-terminal prenylation. Immobilized GST-fusion proteins were incubated with prenylated Rho3 or Cdc42 obtained from the in vitro translation described in *Materials and Methods*. Input lanes for Rho3 binding experiments represent signal equivalent to 2.5% binding. Input lane for Cdc42 binding experiments represent signal equivalent to 10% binding. The Cdc42-N17 binding experiment was exposed to film twice as long as the other experiments due to lower efficiency of translation for this mutant.

with recombinant Rho3 reflects only a residual level of interaction seen with the modified form of the protein.

To further examine the apparent requirement for CAAX prenylation in the interaction between these Rho GTPases and Exo70, we made use of rabbit reticulocyte lysates that have been shown to be active in prenylating CAAX motifs in vitro (Hancock, 1995). We examined whether we could detect prenylation of either yeast GTPase after in vitro translation. When Rho3-L74 (GTP) or Rho3-N30 (GDP) were translated in reticulocyte lysates and further incubated for 6 h, a faster migrating form of the protein appeared over time. When activated Rho3 containing a mutation of the critical cysteine (C228) in the CAAX motif was used, the faster migrating form failed to appear (Figure 4B). The addition of mevalonic acid—a metabolic precursor of both farnesyl and geranylgeranyl moieties used to modify CAAX motifs—has been shown to stimulate both types of prenylation in reticulocyte lysates. As can be seen from Figure 4B, the addition of mevalonic acid to the reaction after translation results in a dramatic increase in the conversion of Rho3-L74 and Rho3-N30 proteins to the faster migrating form but has no effect on the Rho3-L74,A228 mutant lacking the prenylation acceptor cysteine.

We examined the ability of in vitro prenylated Rho3 from reticulocyte lysates to bind to GST-Exo70 under conditions similar to that used for the yeast lysate binding studies described above. The results show that in vitro prenylated Rho3-L74 (GTP-locked) binds well to the GST-Exo70, whereas prenylated Rho3-N30 (GDP form) fails to bind (Figure 4C). Importantly, only very weak binding is seen when unprenylated but activated Rho3-L74,A228 is present. Un-

like Rho3, we were unable to detect a cysteine-dependent mobility shift in a parallel set of translations with Cdc42 translated in the reticulocyte system. However, when we examined the binding of translations of activated Cdc42 (Cdc42L61) in the presence or absence of mevalonate and the presence or absence of the C-terminal cysteine we find that binding to Exo70 is dependent on GTP, the addition of mevalonate, and the CAAX box. This provides strong evidence that, like Rho3, prenylation of Cdc42 CAAX motif is required for interaction with Exo70 in this system. Together with the binding assays using GTPases from yeast lysates, these data clearly demonstrate that prenylation of Rho3 and Cdc42 is an important determinate in promoting the binding between these Rho GTPase and Exo70.

Binding of Prenylated Rho3 and Cdc42 to Exo70 Is Not Dependent on the C Domain

Previous studies to map the site of Rho3 interaction within Exo70 depended largely on the use of recombinant (i.e., unprenylated) forms of Rho3. These studies identified an important role for C domain of Exo70 in mediating the interaction with recombinant Rho3. Either mutations in, or deletion of, C domain of Exo70 result in dramatic loss of binding to Rho3 (Dong *et al.*, 2005; He *et al.*, 2007b; Hutagalung *et al.*, 2009). To determine whether prenylated Rho3 and Cdc42 were similarly dependent on the Exo70 C domain for their interaction, we made use of two mutant forms of Exo70, Exo70-1521 and Exo70-ΔC. Exo70-1521 has a combination of six alanine substitutions in surface exposed residues within the C domain that block binding to recombinant Rho3 (He *et al.*, 2007b), and Exo70-ΔC mutant contains a replacement of the entire C domain with an
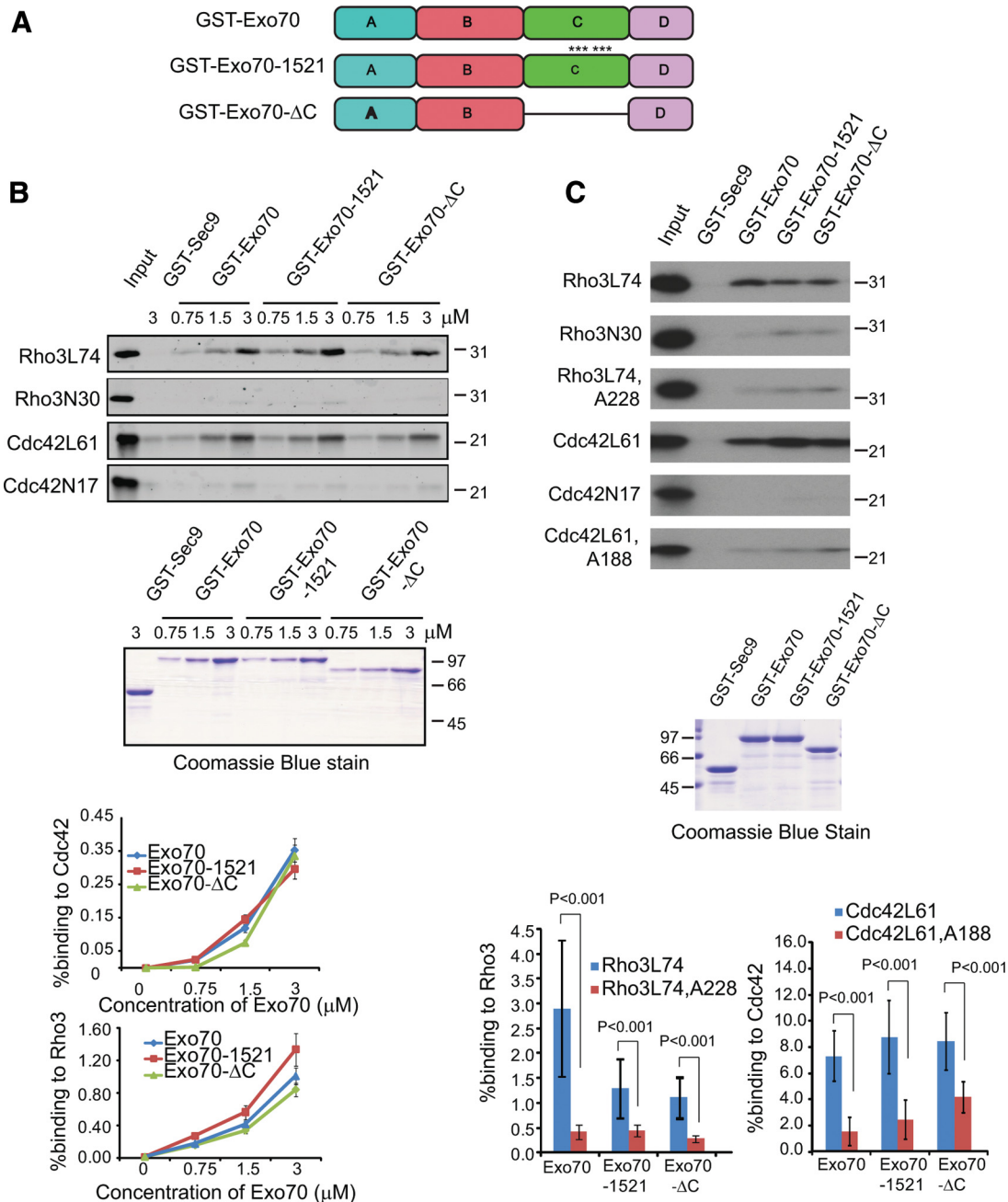
Figure 5. Binding of prenylated Rho3 and Cdc42 to Exo70 does not depend on C domain. (A) Schematics of the Exo70-1521 mutation and a domain C deletion. (B) Mutations in or a deletion of Exo70 domain C does not significantly affect the interaction between Exo70 and Rho3 or Cdc42 produced in yeast. Yeast lysates from cells overexpressing GTP or GDP locked Rho3 and Cdc42 were incubated with immobilized GST-fusion proteins at different concentrations. Binding experiments were performed as described in *Materials and Methods*. Graphs represent quantitation of the binding with error bars representing SD of three independent experiments. (C) Mutations in or a deletion of Exo70 domain C does not significantly affect the interaction between Exo70 and Rho3 or Cdc42 prenylated in vitro after translation in reticulocyte lysates. Immobilized GST proteins were incubated with prenylated Rho3 and Cdc42 obtained from the in vitro translation as described in *Materials and Methods*. Input lanes for Rho3 binding experiments represent signal equivalent to 2.5% binding. Input lane for Cdc42 binding experiments represent signal equivalent to 10% binding. The Cdc42-N17 binding experiment was exposed to film twice as long as the other experiments due to lower efficiency of translation for this mutant. Shown below is Coomassie Blue staining of the GST fusion proteins used for binding and bar graphs representing quantitation of the binding with error bars representing SD of three independent experiments.

eight residue flexible linker (Hutagalung *et al.*, 2009). We compared the binding of these two forms of Exo70 fused to GST to equivalent amounts of wild-type full-length Exo70 by using the Rho GTPases produced in yeast lysates. Remarkably, we found that both GST-Exo70-1521 and GST-Exo70-ΔC mutant proteins

showed binding activity to yeast Rho3-L74 and Cdc42-L61 that was indistinguishable from that of wild-type Exo70 (Figure 5B). As before, this binding was highly dependent on the activation status of the Rho3 and Cdc42. We repeated these binding assays using the in vitro translated/in vitro preny-

lated Rho3 protein. Using the in vitro modified Rho3, we see a small loss of binding activity to the GST-Exo70-1521 and GST-Exo70-ΔC mutant proteins, but both mutants demonstrate very clear binding which is highly dependent on both the activation (i.e., GTP) and prenylation status of Rho3. Therefore, both of these assays reveal that Exo70 is able to interact with Rho GTPases in a manner that does not depend on the C domain and that the prenylation state of these GTPases seems to be critical in revealing this mode of interaction. It is worth noting that mammalian TC10 GTPase (produced in NIH 3T3 cells and hence probably prenylated) also has been shown to interact with mammalian Exo70 in a manner that does not depend of the C domain (Chiang *et al.*, 2001).

Isolation of Novel Conditional-Lethal Alleles of EXO70

A previous screen for mutants in *EXO70* resulted in the identification of two alleles, *exo70-38* and *exo70-35*, with unusual phenotypes nearly identical to those described for *cdc42-6* (He *et al.*, 2007a). Like *cdc42-6* mutants, *exo70-38* and *exo70-35*, exhibit defects in secretion of Bgl2 but not invertase and show accumulation of post-Golgi vesicles in small-but not large-budded cells. Invertase and Bgl2 are thought to be delivered to the cell surface through two distinct populations of post-Golgi vesicles, and both populations are blocked by all of the original 10 late *sec* mutants (Harsay and Bretscher, 1995). The remarkable similarity of the unusual phenotypes of the *exo70-38* and *exo70-35* mutants with the *cdc42-6* mutant gives strong in vivo support for the notion that Exo70 is a direct effector of Cdc42 function in exocytosis, as suggested by the dominant suppressor and biochemical interaction studies described above. However, the phenotypes associated with the *exo70-38* and *exo70-35* mutants are not consistent with the model that Exo70 is a downstream effector of the Rho3 GTPase. The *rho3-V51* mutant has significantly more expansive secretory defects than seen in these two mutants. Specifically, the *rho3-V51* mutant shows pronounced defects in both invertase and Bgl2 secretion and accumulates post-Golgi vesicles in both small and large budded cells. Because these phenotypes are at odds with the genetic and biochemical studies described above linking Exo70 as a downstream effector of both GTPases, we postulated that the *exo70-38* and *exo70-35* mutants might represent hypomorphic alleles of *EXO70*, defective in transmitting Cdc42 function but still permissive for promoting Rho3 function. To test this idea, we set out to identify and characterize novel conditional-lethal alleles in *EXO70* and describe the loss-of-function phenotoypes associated with them.

To identify additional alleles of *EXO70* with recessive conditional growth defects, we screened a library of random PCR-generated *exo70* mutants by using a plasmid shuffle strategy (see *Materials and Methods*). After growth on 5-FOA media at 25°C (to evict the *EXO70* plasmid and reveal possible recessive phenotypes), 57 independent colonies were identified that exhibited low-temperature–sensitive growth at 14°C (cs−), and 40 colonies were identified that exhibited high-temperature–sensitive (ts−) growth. After recovery of the mutant plasmids from these strains and retransformation into the *exo70Δ/CEN-URA3-EXO70* plasmid shuffle strain, we identified one plasmid containing a cold-sensitive allele (*exo70-188*), and one plasmid containing a temperature-sensitive allele (*exo70-113*). These alleles (as well as wild-type *EXO70* control) were then integrated at the *EXO70* locus by replacing a disruption in a heterozygous diploid. After sporulation and tetrad dissection, the pattern of spores showing conditional growth was seen to be tightly linked to the newly introduced allele. Thus the phenotypes of the integrated alleles were similar to that of the original plasmid-borne mutants. These integrated mutant strains were then used for all the subsequent analyses of the growth and secretion phenotypes associated with these new alleles of *exo70*.

We examined the *exo70-188*$^{cs-}$ allele for its ability to secrete invertase and Bgl2 at permissive temperature (25°C) and after a 9-h shift to the nonpermissive conditions (14°C). A wild-type *EXO70* and cold-sensitive *rho3-V51* strain were assayed in parallel as negative and positive controls for cold-sensitive secretory defects. As can be seen in Figure 6, B and C, the *exo70-188* mutant shows pronounced invertase and Bgl2 secretion defects at 14°C (relative to *EXO70*), and both the magnitude and temperature dependence of these secretory effects are remarkably similar to that seen in *rho3-V51* cells (Roumanie *et al.*, 2005). When *exo70-188* cells were shifted to 14°C and then examined by thin-section electron microscopy, a highly penetrant (>80% of cells) and dramatic (>75 vesicles/cell on average) accumulation of 80- to 100-nm post-Golgi vesicles was apparent (Figure 6, D and E). As we had seen previously with *rho3-V51*, and consistent with the secretion data, a lower—and less penetrant—level of vesicle accumulation was observed in *exo70-188* mutants grown at the permissive temperatures (Figure 6, D and E). To determine whether there was an effect of the stage of the cell cycle on vesicle accumulation in this mutant, we compared the vesicle accumulation in cells with small (<1-μm-diameter) buds compared with larger (>1-μm-diameter) buds, as we have previously with *cdc42-6* and *exo70-38*. The results, shown in Figure 6D clearly demonstrate that both large- and small budded *exo70-188* cells have a similar high degree of penetrance and vesicle accumulation at both permissive and nonpermissive temperatures.

The temperature-sensitive *exo70-113* mutant was characterized in a similar manner except that cells were shifted to 37°C for 2 h to examine the effect of temperature-shift on exocytic function. An isogenic wild-type *EXO70* and *sec6-4* mutant were examined in parallel as controls. As can be seen in Figure 7, B and C, the *exo70-113*$^{ts-}$ mutant shows pronounced invertase and Bgl2 secretion defects after a shift to 37°C and when examined by thin section electron microscopy, a highly penetrant (>80% of cells) and strong (>80 vesicles/cell, on average) accumulation of 80- to 100-nm post-Golgi vesicles was apparent in both large- and small-budded cells (Figure 7, D and E). Together, our analysis of these two new alleles demonstrates that Exo70 function is required for all the secretory functions seen with other late-acting *sec* genes including secretion of both the Bgl2 and the invertase class of vesicles, and exocytosis in early bud emergence as well as in later stages of bud growth. These observations are important to the present study because they demonstrate that the spectrum of phenotoypes associated with loss-of Exo70 function is entirely consistent with Exo70 being a downstream effector of both Cdc42 and Rho3 function in exocytosis.

DISCUSSION

We have previously characterized a role for Cdc42 and Rho3 as positive regulators of exocytosis and found that this role was independent of polarization of both the actin cytoskeleton and of the exocyst complex (Roumanie *et al.*, 2005). We suggested a model where these GTPases would work by locally increasing the activity (or throughput) of the exocytic apparatus at sites occupied by GTP-bound Rho/Cdc42 proteins (Roumanie *et al.*, 2005; Wu *et al.*, 2008). However, the precise effector pathway by which such a mechanism would take place was either unknown—as for Cdc42—or highly controversial—as for Rho3. In this report, we provide three independent lines of evidence that strongly supports this model of regulation and demon-
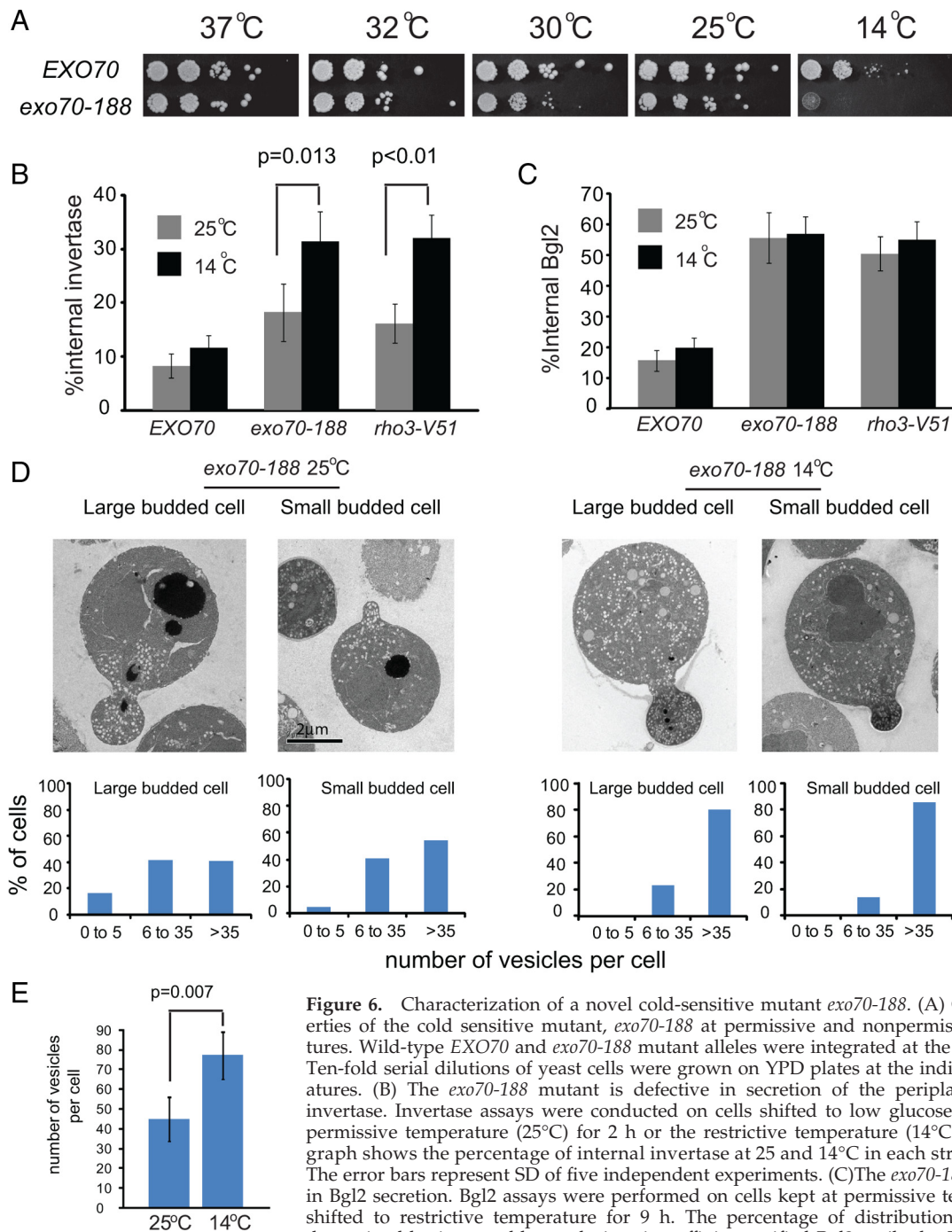
Figure 6. Characterization of a novel cold-sensitive mutant *exo70-188*. (A) Growth properties of the cold sensitive mutant, *exo70-188* at permissive and nonpermissive temperatures. Wild-type *EXO70* and *exo70-188* mutant alleles were integrated at the *EXO70* locus. Ten-fold serial dilutions of yeast cells were grown on YPD plates at the indicated temperatures. (B) The *exo70-188* mutant is defective in secretion of the periplasmic enzyme invertase. Invertase assays were conducted on cells shifted to low glucose media at the permissive temperature (25°C) for 2 h or the restrictive temperature (14°C) for 9 h. The graph shows the percentage of internal invertase at 25 and 14°C in each strain analyzed. The error bars represent SD of five independent experiments. (C)The *exo70-188* is defective in Bgl2 secretion. Bgl2 assays were performed on cells kept at permissive temperature or shifted to restrictive temperature for 9 h. The percentage of distribution of Bgl2 was determined by immunoblot analysis using affinity-purified Bgl2 antibody. The graph depicts the percentage of Bgl2 protein that remains internal in *EXO70*, *exo70-188*, and *rho3-V51* strains. Quantitations were performed by Odyssey infrared imaging system. Error bars represent SD of four independent experiments. (D) The *exo70-188* mutant accumulates post-Golgi vesicles in both large-budded cells and small-budded cells. The *exo70-188* mutant cells kept at the permissive temperature or shifted to restrictive temperature for 9 h were fixed and processed for electron microscopy. Examples of both small- (<1-μm) and large-budded (≥1-μm) cells are shown. Cells were scored for number of vesicles accumulated throughout the cell and bar graphs show the percentage of small-budded or large-budded cells containing different number of vesicles. Bar, 2 μm. (E) Overall post-Golgi vesicle accumulation was determined for electron microscopy sections by scoring cells >3 μm in diameter (irrespective of bud or bud size) for 80- to 100-nm vesicles. For each condition, micrographs were divided into three groups representing 20–25 cells each to determine the SD in this assay.

strates that the Exo70 component of the exocyst complex represents a critical and direct effector for both Rho3 and Cdc42 function in spatial regulation of exocytosis.

Several studies have been carried out to investigate the interaction of Exo70 and Rho family GTPases in yeast and mammalian cells. However, despite the fact that both yeast and mammalian Exo70 have been reported to bind Rho family GTPases and the overall structural similarity between yeast and mammalian Exo70 proteins is very high throughout their length, the sites of interaction reported for the
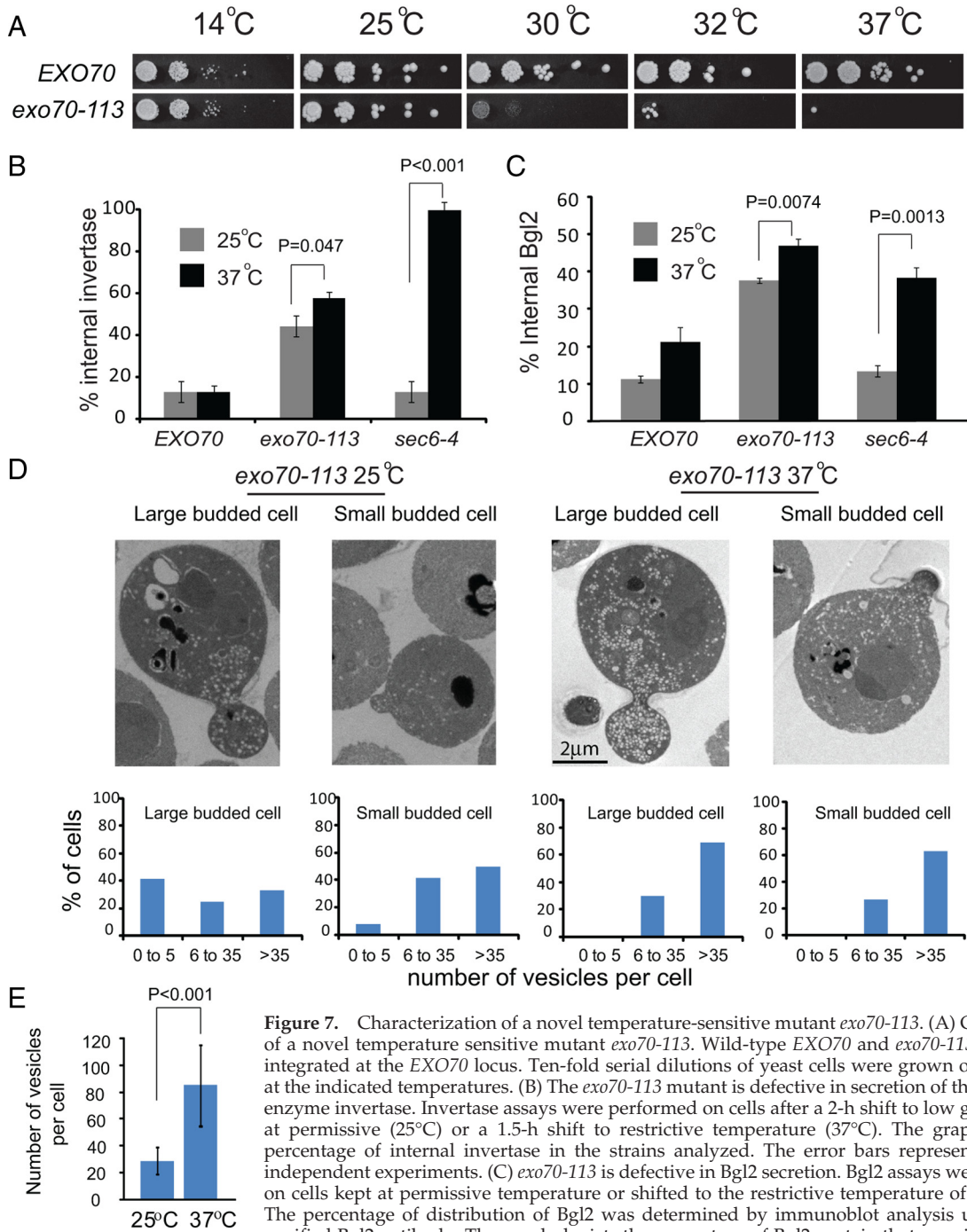
Figure 7. Characterization of a novel temperature-sensitive mutant *exo70-113*. (A) Growth defect of a novel temperature sensitive mutant *exo70-113*. Wild-type *EXO70* and *exo70-113* alleles were integrated at the *EXO70* locus. Ten-fold serial dilutions of yeast cells were grown on YPD plates at the indicated temperatures. (B) The *exo70-113* mutant is defective in secretion of the periplasmic enzyme invertase. Invertase assays were performed on cells after a 2-h shift to low glucose media at permissive (25°C) or a 1.5-h shift to restrictive temperature (37°C). The graph shows the percentage of internal invertase in the strains analyzed. The error bars represent SD of four independent experiments. (C) *exo70-113* is defective in Bgl2 secretion. Bgl2 assays were performed on cells kept at permissive temperature or shifted to the restrictive temperature of 37°C for 2 h. The percentage of distribution of Bgl2 was determined by immunoblot analysis using affinity-purified Bgl2 antibody. The graph depicts the percentage of Bgl2 protein that remains internal in *EXO70*, *exo70-113*, and *sec6-4* strains. Quantitations were performed by Odyssey infrared imaging system. Error bars represent SD of four independent experiments. (D) *exo70-113* mutant accumulates post-Golgi vesicles in both large-budded cells and small-budded cells. *exo70-113* mutant cells kept at the permissive temperature or shifted to restrictive temperature for 2 h were fixed and processed for electron microscopy. Examples of both small- (<1-μm) and large-budded (≥ 1 μm) cells are shown. Cells were scored for number of vesicles accumulated throughout the cell, and bar graphs show the percentage of small-budded or large-budded cells containing different number of vesicles. Bar, 2 μm. (E) Overall post-Golgi vesicle accumulation was determined for electron microscopy sections by scoring cells >3 μm in diameter (irrespective of bud or bud size) for 80- to 100-nm vesicles.

GTPases seemed to be quite distinct. Studies using tagged-TC10 in transfected mammalian cells identified a region within domains A and B in mouse Exo70 as the major site of binding, whereas studies using recombinant Rho3 have identified a binding site within C domain as the major binding site for the yeast Exo70 protein (Dong *et al.*, 2005; He *et al.*, 2007b; Hutagalung *et al.*, 2009). To make matters more difficult, mutations or deletions in Exo70 that block recombinant Rho3 binding had little or no effect on growth or secretion of yeast cells containing these mutant *exo70* alleles as the sole source of Exo70 in the cell (He *et al.*, 2007b; Hutagalung *et al.*, 2009). Finally, phenotypic analysis of two

conditional alleles of *exo70* showed exocytic phenotypes that were remarkably similar to that of *cdc42-6* but very distinct from that of *rho3-V51* (He *et al.*, 2007a). However, despite the similarity in phenotypes with the Cdc42 mutant, biochemical analyses failed to show any detectable interaction between Exo70 and recombinant GTP-bound forms of Cdc42 (He *et al.*, 2007a, this study). Collectively these results seemed to be entirely incompatible with the notion that Exo70 was a direct effector of Cdc42 or Rho3 in yeast. Moreover, the ability of Exo70 family members to interact with Rho GTPases is highly conserved in yeast and mammals, suggesting that structurally divergent mechanisms had evolved into interactions with completely distinct regions of the yeast and mammalian Exo70 proteins.

We have spent considerable effort to find conditions for examining the interaction of Exo70 and either Rho3 or Cdc42 by coimmunoprecipation from detergent lysates. Despite numerous attempts we have been unable to detect this interaction by this method. This may reflect the relatively low affinity of these interactions because, in vivo, these interactions occur on the plasma membrane where the local concentrations of both GTPases and the Exo70 effector are much higher than after lysis in detergent-containing buffer.

A key finding to unraveling these apparently contradictory observations was the use of post-translationally modified forms of Rho3 and Cdc42 in our Exo70 binding studies, a strategy similar to that used to map the TC10 interaction with mammalian Exo70. In particular, we found that mutation of the cysteine present in the C-terminal CAAX motif of either Cdc42 or Rho3 resulted in a dramatic loss of interaction with Exo70. Because this modification does not occur in bacterially-produced forms of these GTPases, the absence of this modification is probably responsible for the dramatic differences seen in the binding assays described here from those described previously. Furthermore, because the mapping of the binding of the Cdc42 homologue TC10 to mouse Exo70 made use of a mammalian expression system (hence, prenylated TC10), this may explain the apparent distinction in the site of binding between the yeast and mammalian forms of Exo70. Further mapping of the Rho GTP binding site in both yeast and mammalian Exo70 will be necessary to determine how structurally similar these binding events are. Because Rho3 and Cdc42 are predicted to be prenylated with different prenyl moieties—Rho3 with farnesyl and Cdc42 with geranlygeranyl—we think it unlikely that the prenyl groups themselves are part of the effector interaction. Rather, we suggest that the presence of the prenyl group is likely to affect presentation of the GTP-bound Rho protein to Exo70 in the context of the detergent micelles present in the binding assays. This may reflect the nature of the interaction that probably occurs in proximity to the membrane in vivo, because both Exo70 and the GTPase have C-terminal membrane-targeting motifs. A role for prenylation in effector binding is unusual but not unprecedented. Ohya and colleagues (Inoue *et al.*, 1999) demonstrated that the physical interaction of Rho1 with its effector Fks1 was highly dependent on the C-terminal geranylgeranylation. It remains to be seen whether other Rho effector relationships depend on prenylation because this is it not a feature that is commonly examined.

What does "activation" of the exocyst by Rho GTPases do to regulate exocytosis? In its simplest form, this activation would involve an increase in the rate of vesicle docking and fusion at a specific place on the plasma membrane demarcated by the GTP-bound form of Cdc42 and/or Rho3. Because the loss of function mutants in *cdc42* and *rho3* fail to show a detectable effect on polarization of Sec4 or exocyst

subunits to sites of polarized growth, and the mutants are strongly suppressed by increased levels of the target membrane-soluble *N*-ethylmaleimide-sensitive factor attachment protein receptor (SNARE) Sec9, we favor the model that these GTPases act through the exocyst to increase localized SNARE assembly leading to more rapid vesicle fusion. The details of how this activation mechanism works remain to be elucidated. However, because dominant alleles of Exo70 described here act as though they are "constitutively active" forms of Exo70they will be valuable tools in helping to understand the nature of this activation. For example, all of the gain-of-function mutants seem to have similarly fully assembled exocyst complex, suggesting that assembly and/or disassembly of the complex is unlikely to represent the major mode of regulation by these GTPases.

In addition to Exo70, Sec3—another component of the exocyst complex—has been proposed to be an effector in regulating polarized growth downstream of the Rho1 and Cdc42 GTPases (Guo *et al.*, 2001; Zhang *et al.*, 2008; Hutagalung *et al.*, 2009). However, it is unlikely that Sec3 is the principal effector for Cdc42 function in exocytosis. First, deletion of the N-terminal Rho-binding domain of Sec3 is nonessential and has no detectable impact on polarized growth or secretion at any temperature, whereas the *cdc42-6* mutant results in a severe temperature-sensitive growth and secretion defect. Second, we have shown previously that deletion of the Sec3 N-terminal domain results in a synthetic lethal phenotype when combined with the *cdc42-6* mutant, which strongly suggests that this domain of Sec3 has an important role that acts in parallel (perhaps through Rho1 signaling) with Cdc42 signaling through Exo70 (Roumanie *et al.*, 2005). In agreement with the idea that the Cdc42–Exo70 pathway functions in parallel with a Sec3–Rho pathway, several groups have shown synthetic lethality between *sec3-DNT* and several *EXO70* loss-of-function mutants (Zhang *et al.*, 2008; Hutagalung *et al.*, 2009). It also important to note that although the Exo70 effector activity seems to be regulated by both Rho3 and Cdc42 but not Rho1, the N terminus of Sec3 has been reported to interact with both Rho1 and Cdc42 but not Rho3. Therefore, this process seems to be regulated by a complex network of partially overlapping Rho GTPase/effector relationships which may provide increased robustness to the overall spatial regulation of polarized exocytosis.

REFERENCES

Adamo, J. E., Moskow, J. J., Gladfelter, A. S., Viterbo, D., Lew, D. J., and Brennwald, P. J. (2001). Yeast Cdc42 functions at a late step in exocytosis, specifically during polarized growth of the emerging bud. J. Cell Biol. *155*, 581–592.

Adamo, J. E., Rossi, G., and Brennwald, P. (1999). The Rho GTPase Rho3 has a direct role in exocytosis that is distinct from its role in actin polarity. Mol. Biol. Cell *10*, 4121–4133.

Bradford, M. M. (1976). A rapid and sensitive method for the quantitation of microgram quantities of protein utilizing the principle of protein-dye binding. Anal. Biochem. *72*, 248–254.

Chiang, S. H., Baumann, C. A., Kanzaki, M., Thurmond, D. C., Watson, R. T., Neudauer, C. L., Macara, I. G., Pessin, J. E., and Saltiel, A. R. (2001). Insulin-stimulated GLUT4 translocation requires the CAP-dependent activation of TC10. Nature *410*, 944–948.

Dong, G., Hutagalung, A. H., Fu, C., Novick, P., and Reinisch, K. M. (2005). The structures of exocyst subunit Exo70p and the Exo84p C-terminal domains reveal a common motif. Nat. Struct. Mol. Biol. *12*, 1094–1100.

Guo, W., Roth, D., Walch-Solimena, C., and Novick, P. (1999). The exocyst is an effector for Sec4p, targeting secretory vesicles to sites of exocytosis. EMBO J. *18*, 1071–1080.

Guo, W., Tamanoi, F., and Novick, P. (2001). Spatial regulation of the exocyst complex by Rho1 GTPase. Nat. Cell Biol. *3*, 353–360.

Guthrie, C., and Fink, G. (1991). Guide to Yeast Genetics and Molecular Biology, Methods in Enzymology, San Diego, CA: Academic Press.

Hamburger, Z. A., Hamburger, A. E., West, A. P., Jr., and Weis, W. I. (2006). Crystal structure of the *S. cerevisiae* exocyst component Exo70p. J. Mol. Biol. *356*, 9–21.

Hancock, J. F. (1995). Reticulocyte lysate assay for in vitro translation and posttranslational modification of Ras proteins. Methods Enzymol. *255*, 60–65.

Harsay, E., and Bretscher, A. (1995). Parallel secretory pathways to the cell surface in yeast. J. Cell Biol. *131*, 297–310.

He, B., Xi, F., Zhang, J., TerBush, D., Zhang, X., and Guo, W. (2007a). Exo70p mediates the secretion of specific exocytic vesicles at early stages of the cell cycle for polarized cell growth. J. Cell Biol. *176*, 771–777.

He, B., Xi, F., Zhang, X., Zhang, J., and Guo, W. (2007b). Exo70 interacts with phospholipids and mediates the targeting of the exocyst to the plasma membrane. EMBO J. *26*, 4053–4065.

Hsu, S. C., TerBush, D., Abraham, M., and Guo, W. (2004). The exocyst complex in polarized exocytosis. Int. Rev. Cytol. *233*, 243–265.

Hutagalung, A. H., Coleman, J., Pypaert, M., and Novick, P. J. (2009). An internal domain of Exo70p is required for actin-independent localization and mediates assembly of specific exocyst components. Mol. Biol. Cell *20*, 153–163.

Imai, J., Toh-e, A., and Matsui, Y. (1996). Genetic analysis of the *Saccharomyces cerevisiae* RHO3 gene, encoding a rho-type small GTPase, provides evidence for a role in bud formation. Genetics *142*, 359–369.

Inoue, S. B., Qadota, H., Arisawa, M., Watanabe, T., and Ohya, Y. (1999). Prenylation of Rho1p is required for activation of yeast 1,3-beta-glucan synthase. J. Biol. Chem. *274*, 38119–38124.

Lehman, K., Rossi, G., Adamo, J. E., and Brennwald, P. (1999). Yeast homologues of tomosyn and lethal giant larvae function in exocytosis and are associated with the plasma membrane SNARE, Sec9. J. Cell Biol. *146*, 125–140.

Matsui, Y., and Toh, E. A. (1992). Yeast RHO3 and RHO4 ras superfamily genes are necessary for bud growth, and their defect is suppressed by a high dose of bud formation genes CDC42 and BEM1. Mol. Cell. Biol. *12*, 5690–5699.

Moore, B. A., Robinson, H. H., and Xu, Z. (2007). The crystal structure of mouse Exo70 reveals unique features of the mammalian exocyst. J. Mol. Biol. *371*, 410–421.

Munson, M., and Novick, P. (2006). The exocyst defrocked, a framework of rods revealed. Nat. Struct. Mol. Biol. *13*, 577–581.

Nelson, W. J., and Yeaman, C. (2001). Protein trafficking in the exocytic pathway of polarized epithelial cells. Trends Cell Biol. *12*, 483–486.

Robinson, N. G., Guo, L., Imai, J., Toh, E. A., Matsui, Y., and Tamanoi, F. (1999). Rho3 of *Saccharomyces cerevisiae*, which regulates the actin cytoskeleton and exocytosis, is a GTPase which interacts with Myo2 and Exo70. Mol. Cell. Biol. *19*, 3580–3587.

Roumanie, O., Wu, H., Molk, J. N., Rossi, G., Bloom, K., and Brennwald, P. (2005). Rho GTPase regulation of exocytosis in yeast is independent of GTP hydrolysis and polarization of the exocyst complex. J. Cell Biol. *170*, 583–594.

Sivaram, M. V., Furgason, M. L., Brewer, D. N., and Munson, M. (2006). The structure of the exocyst subunit Sec6p defines a conserved architecture with diverse roles. Nat. Struct. Mol. Biol. *13*, 555–556.

TerBush, D. R., and Novick, P. (1995). Sec6, Sec8, and Sec15 are components of a multisubunit complex which localizes to small bud tips in *Saccharomyces cerevisiae*. J. Cell Biol. *130*, 299–312.

Wu, H., Rossi, G., and Brennwald, P. (2008). The ghost in the machine: small GTPases as spatial regulators of exocytosis. Trends Cell Biol. *18*, 397–404.

Zhang, X., Orlando, K., He, B., Xi, F., Zhang, J., Zajac, A., and Guo, W. (2008). Membrane association and functional regulation of Sec3 by phospholipids and Cdc42. J. Cell Biol. *180*, 145–158.